

**OPEN ACCESS**

## Analysis of EUV spectra from highly charged iron ions with a compact EBIT

To cite this article: N Yamamoto *et al* 2009 *J. Phys.: Conf. Ser.* **163** 012023

View the [article online](#) for updates and enhancements.

### You may also like

- [Copenhagen Plus: Complementing output oriented climate policy by input oriented approaches](#)

H-J Luhmann and Stefan Lechtenbohmer

- [Unstable quantum oscillator](#)

M G Espinosa and P Kielanowski

- [A finance architecture for technology development and transfer](#)

Heleen de Coninck, A Higham and E Hailes

The advertisement features a green background on the left with the ECS logo and text. The right side has a dark teal background with white text and images of industrial robotics and a scientist.

**ECS**  
The  
Electrochemical  
Society  
Advancing solid state &  
electrochemical science & technology

**DISCOVER**  
how sustainability  
intersects with  
electrochemistry & solid  
state science research

# ANALYSIS OF EUV SPECTRA FROM HIGHLY CHARGED IRON IONS WITH A COMPACT EBIT

N. Yamamoto<sup>1</sup>, H. A. Sakaue<sup>2</sup>, D. Kato<sup>2</sup>, I. Murakami<sup>2</sup>, T. Kato<sup>2</sup>,

N. Nakamura<sup>3</sup>, E. Watanabe<sup>3</sup> H. Nishimura<sup>1</sup> and T. Watanabe<sup>4</sup>

<sup>1</sup> Institute of Laser Engineering, Osaka University, Suita, Osaka 565-0871, Japan

<sup>2</sup> National Institute for Fusion Science, Toki, Gifu 509-5292, Japan

<sup>3</sup> Institute for Laser Science, The University of Electro-Communications, Chofu, Tokyo 182-8585, Japan

<sup>4</sup> National Astronomical Observatory of Japan, Mitaka, Tokyo, 181-8588, Japan

yamamoto-no@ile.osaka-u.ac.jp

**Abstract.** For benchmark tests of the spectral analysis tool for solar plasma, applying the theoretical plasma radiation model to the laboratory plasma is important. In this paper, a compact-EBIT (Electron Beam Ion Trap) was adopted as the laboratory plasma, and extreme UV spectra of Fe ions were measured by the flat-field grazing-incidence spectrometer with no slit. In order to analyze the spectra from plasma generated by mono-energetic electron beam, our model was revised in term of an electron velocity distribution. Consequently, the measured spectra by the compact-EBIT were analyzed by our revised model.

## 1. Introduction

Solar observations have been progressed by HINODE satellite that was launched on 2006 September 23 JST [1]. HINODE satellite has a high precise spectrometer EIS (EUV Imaging Spectrometer). EIS measure EUV spectra in the range of 170-210Å and 250-290Å. In these wavelength ranges, many M-shell Fe ion lines and some L-shell ion lines are measured. These ions are found in the electron temperature of several ten eV to few hundred eV (few keV in flare). M-shell Fe ion lines are often applied for density diagnostics in the region between transition and corona of the Sun. Therefore, the plasma diagnostic tool for line intensity analysis is important and the tool should be evaluated by applying to some laboratory plasmas where the parameters are under control.

In the previous study, the benchmark tests by CHIANTI code [2] and our original model including the most recent atomic data have been carried out by applying to EIS's spectra from solar plasma [3]. Our model was also applied to LHD (large helical device) plasma at NIFS (National Institute for Fusion Science) as the benchmark test [4]. In this study, spectra measured by an EBIT (electron beam ion trap) [5] are adopted as a benchmark test. The generated plasma by EBIT has a simpler plasma parameter profile than magnetic confined plasma. However, an electron energy of the Tokyo-EBIT is much too high to produce M-shell iron ions. Therefore we build a new compact-EBIT [6]. In this paper, we present the analysis of the first data obtained with the compact-EBIT.

## 2. Experiments

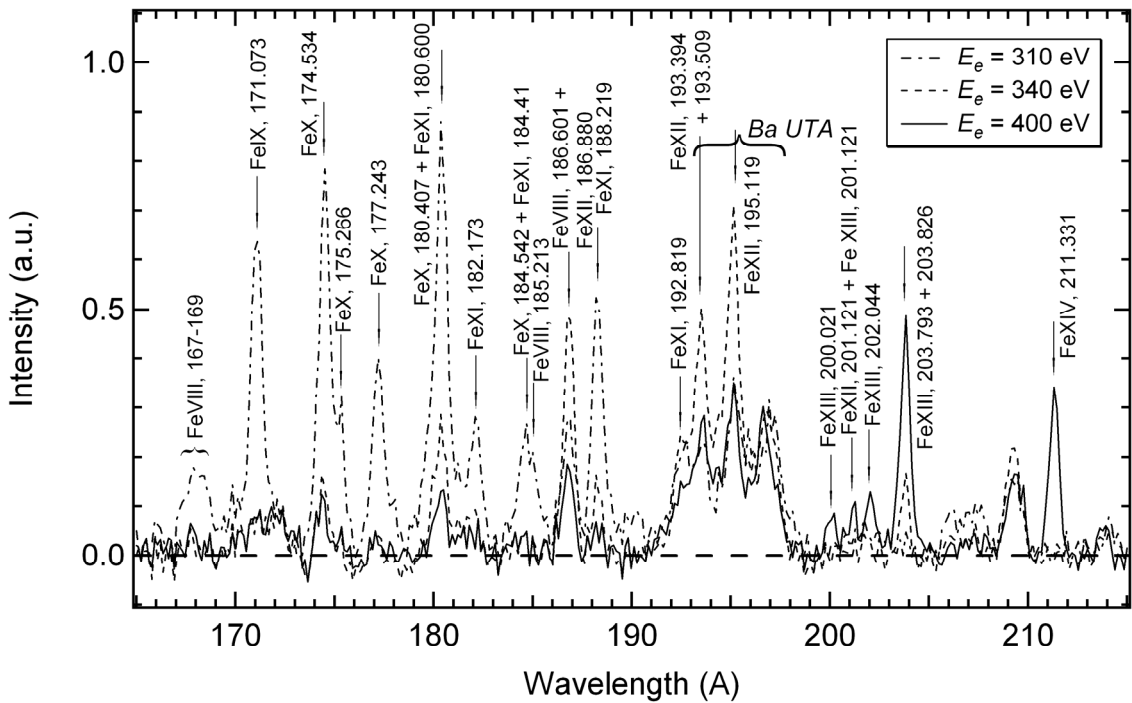


**Figure 1.** The measured spectra by the compact-EBIT for different electron energy with line identifications. Solid, dashed and dot-dashed lines are spectra by electron beam energy  $E_e$  of 400 eV, 340 eV and 310 eV, respectively.

The compact-EBIT was developed in order to generate plasmas at lower electron energies than in the Tokyo-EBIT. The experimental setup and conditions are found in ref. [7]. In these experiments, Fe was injected by using ferrocene ( $\text{Fe}(\text{C}_5\text{H}_5)_2$ ). The flat-field grazing-incidence spectrometer with no slit consists of 1200 grooves/mm laminar-type replica diffraction grating (30-002, Shimazu Corporation) and the back-illuminated CCD camera (Princeton Instruments PIXIS-XO:400B). EUV spectra in the range of 130-300 Å can be measured by the spectrometer.

Figure 1 shows the measured spectra at electron energy of 310 eV, 340 eV and 400 eV. The electron current of the cathode in the compact-EBIT is 20mA. With decreasing electron energy, spectral lines of lower ionized ions become strong. Spectral resolution of the present spectra was FWHM  $\sim 0.83$  Å by Gaussian function fitting of some lines. Since the spectrometer has no slit, the resolution depends on plasma size of the compact-EBIT. Spectral lines were identified by using the line database of NIST [8] and CHIANTI. In the measured spectra by electron energy of 310 eV, lines of Fe IX-XI are strong. Broad lines of 192-198 Å belong to a UTA (Unresolved Transition Array) of Ba ions from the cathode.

### 3. Collisional-radiative model

#### 3.1. Electron velocity distribution

We had constructed a collisional-radiative model for Fe ion lines analysis [4]. In this study, we revised the model about electron velocity distribution for spectra analysis of the EBIT. An electron velocity in the compact-EBIT has a vector of the beam direction and electron energy is monochromatic, i.e. it has no temperature. It means that electron velocity distribution to calculate transition rates is not Maxwellian distribution. As electron velocity distribution  $f$ , delta function,

$$f(v) = \delta(v - v_e) \quad (1)$$

was adopted, where  $v_e$  is electron velocity at electron beam energy of  $E_e$ . The rate coefficient  $C_e$  on the velocity average of a cross section  $\sigma$  is  $C_e = \langle v\sigma \rangle = v_e \sigma(v_e)$  and the formula becomes very simple.

### 3.2. Atomic data

Our model includes the following number of energy levels with fine structure: 1073 for Fe VIII, 1084 for Fe IX, 1189 for Fe X, 1287 for Fe XI, 917 for Fe XII, 332 for Fe XIII and 243 for Fe XIV ( $3 \leq n \leq 5$  &  $0 \leq l \leq 4$ ). Level energies of lower excited states ( $n \leq 3$ ) were corrected by NIST database. Atomic data were calculated by HULLAC code [9]. Since the electron velocity distribution is a delta function, cross sections at beam energy are important. The effects of resonance in the excitation cross section at threshold energy range do not affect excitation rates. Therefore we did not use cross sections by the recent relative R-matrix calculation. On the other hand, for radiative transition rates the data of the recent relative R-matrix calculation (ref. [10] for Fe X, ref. [11] for Fe XI and ref. [12] for Fe XIII) were used. In our model, atomic processes include excitation / de-excitation / ionization by electron impact, radiative transition, radiative recombination, three-body recombination.

### 3.3. Rate equation and quasi-steady state solutions

The spectral line intensity is calculated by using the population density  $N_i$  of an excited states  $i$  under certain conditions. The population density is determined by including various atomic processes. The population densities are derived as follows,

$$\frac{dN_i}{dt} = -N_i \sum_j W_{ij} + \sum_j W_{ji} N_j = 0 \quad (2)$$

where  $W_{ij}$  is total transition rate from an  $i$ -state to a  $j$ -state. The population density is able to re-write as

$$N_i = r_i^{ion} N_e N_Z + r_i^{rec} N_e N_{Z+1} \quad (3)$$

where  $r_i^{ion}$  and  $r_i^{rec}$  are population density coefficients of ionization and recombination components,  $N_Z$  and  $N_{Z+1}$  are ion densities of ionization degree of  $+Z$  and  $+(Z+1)$ , respectively. By eq. (2) and (3), differential equations of  $N_i$  can be changed to differential equations of  $r_i$  and ion densities  $N_Z$  become arbitrary parameters. In this paper, population densities of ionization components only are calculated

## 4. Results and Discussions

Figure 2 shows comparisons of the measured spectra with the calculated spectra. In addition, ion abundances for Fe VIII-XIV based on the calculated spectra are also shown. In the measured spectra with the electron energy of 310 eV, lines of Fe XIII-XIV do not appear. In the range of 165-190Å, line spectral structure can be re-produced by our model. Electron density was estimated by a line ratio, 175.27 / 177.24Å of Fe X. The sum of the ion abundances of Fe X and Fe XI were about 70%. The measured spectra with electron energy of 400 eV have weak lines of Fe VIII-XI. Ion abundance of Fe XII was determined by line of 186.88Å because of UTA of Ba in range of 192-198Å. Electron density was estimated to be  $1-10 \times 10^{10} \text{ cm}^{-3}$  by line intensities of 186.88Å / 195.12Å (with UTA of Ba) of Fe XII and 195.53 (with UTA of Ba) / 203.8Å of Fe XIII. The ion abundance of Fe XIV was the largest, because of electron energy of 400 eV corresponds to ionization energy of Fe XIV. Although line intensities of Fe XIII in the measured spectra by electron energy of 400 eV are strong, the ion abundance of Fe XIII was <10%.

## 5. Summary

In this paper, we identified spectral line of the measured spectra by the compact-EBIT in detail and the measured spectra were fitted by our model for a mono-energetic electron beam. Consequently, electron density and the ion abundance were estimated.

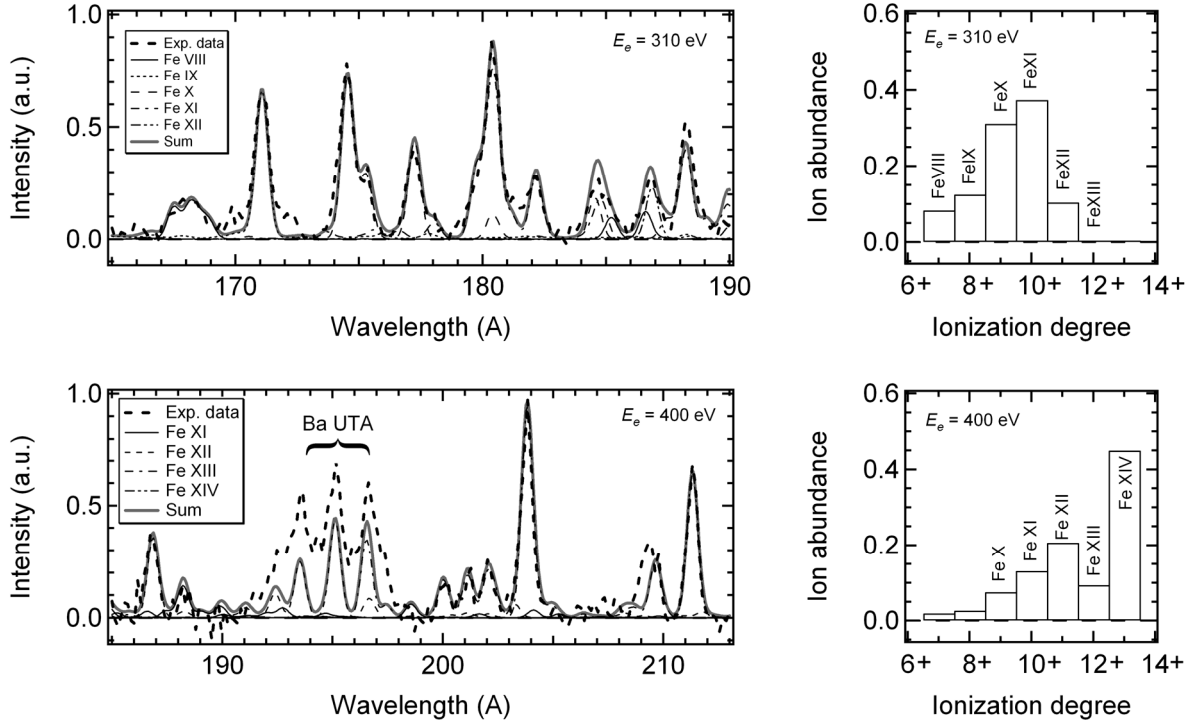


**Figure 2.** Comparison with the measured spectra and the calculated spectra at electron beam energy of 310 eV (top panel) and 400 eV (bottom panel). In the calculated spectra, electron densities are  $1 \times 10^{11} \text{ cm}^{-3}$  for 310 eV and  $5 \times 10^{10} \text{ cm}^{-3}$  for 400 eV (corresponding to electron current of  $\sim 20$  mA). Left figures show comparisons with spectra and right figures show the ion abundance of FeVIII-XIV in calculation by our model.

### Acknowledgements

This work was supported by the Solar and Heliospheric Physics Program of the National Aeronautics and Space Administration under grant NNX07AH986. Travel support was provided by National Science Foundation grant INT-0300708.

### References

- [1] T. Watanabe, et al., Publ. Astron. Soc. Japan **59** S669 (2007).
- [2] G. Del Zanna, et al., CDS Software Note, N. 50 (1997).
- [3] T. Watanabe et al., ApJ., to be published.
- [4] N. Yamamoto et al., ApJ. **689**, 646 (2008).
- [5] R. E. Marrs, M. A. Levine, D. A. Knapp, and J. R. Henderson, Phys Rev. Lett. **60**, 1715 (1988).
- [6] N. Nakamura, H. Kikuchi, H. A. Sakaue, and T. Watanabe, Rev. Sci. Instrum. **79**, 063104 (2008).
- [7] H. A. Sakaue et al. this conference series, submitted.
- [8] T. Shirai, J. Sugar, A. Musgrave and W. L. Wiese, J. Phys. Chem. Ref. Data, Monograph **8** (2000). (NIST online Atomic database ; <http://www.physics.nist.gov/PhysRefData/ASD/>).
- [9] A. Bar-Shalom, M. Klapisch, J. Oreg, J. Quant. Spectr. Rad. Transf. **71**, 179 (2001).
- [10] K. M. Aggarwal and F. P. Keenan, A&A **427**, 763 (2004).
- [11] K. M. Aggarwal and F. P. Keenan, Mon. Not. R. Astron. Soc. **338**, 412 (2003).
- [12] K. M. Aggarwal and F. P. Keenan, A&A **429**, 1117 (2005).